Simple variational approach to the quantum Frenkel-Kontorova model

Choon-Lin Ho[1,*] and Chung-I Chou[2]
[1]*Theory Division, Institute of Particles and Nuclear Studies, High Energy Accelerator Research Organization (KEK), Tsukuba, Ibaraki 305, Japan*
[2]*Institute of Physics, Academia Sinica, Taipei 11529, Taiwan*
(Received 10 July 2000; published 18 December 2000)

We present a simple and complete variational approach to the one-dimensional quantum Frenkel-Kontorova model. Dirac's time-dependent variational principle is adopted together with a Hartree-type many-body trial wave function for the atoms. The single-particle state is assumed to have the Jackiw-Kerman form. We obtain an effective classical Hamiltonian for the system, which is simple enough for a complete numerical solution for the static ground state of the model. Numerical results show that our simple approach captures the essence of the quantum effects first observed in quantum Monte Carlo studies.

DOI: 10.1103/PhysRevE.63.016203 PACS number(s): 05.45.−a, 03.65.Sq, 05.30.Jp, 42.50.Dv

I. INTRODUCTION

The Frenkel-Kontorova (FK) model [1,2] is a simple one-dimensional model used to study incommensurate structures appearing in many condensed-matter systems, such as charge-density waves, magnetic spirals, and adsorbed monolayers [3]. These modulated structures arise as a result of the competition between two or more length scales. The FK model describes a chain of atoms connected by harmonic springs subjected to an external sinusoidal potential. In an important development in the study of the classical FK model, Aubry [4] first made use of the connection between the FK model, the so-called ''standard map,'' and the Kolmogorov-Arnold-Moser (KAM) theorem to reveal many interesting features of the FK model. Particularly, he showed that when the mean distance (also called the winding number) between two successive atoms is rational, the system is always pinned. But when the winding number is irrational, there exits a critical external field strength below (above) which the system is unpinned (pinned). This transition is called by Aubry a ''transition by breaking of analyticity,'' and is closely connected with the breakup of a KAM torus. It is very analogous to a phase transition, and various critical exponents and questions of universality have been extensively studied in the past.

In recent years, the FK model has been applied to the study of transmission in Josephson junction and atomic-scale friction-nanoscale tribology [5]. In these cases, quantum effects are very important. Unlike the classical case, the study of quantum FK models is rather scanty. It was first considered in a quantum Monte Carlo (QMC) analysis in Ref. [6]. Their main observation is that the map appropriate to describe the quantum case is no longer the standard map, but rather a map with a sawtooth shape. Theoretical explanation of this phenomenon was later attempted in Ref. [7]. In this paper the authors first showed that the sawtooth map could not be explained in the naive mean-field approximation (MFA), i.e., the Hartree's independent-particle approximation, which they used. It was then argued that to get the sawtooth map one must go beyond the MFA by including the contributions from the so-called quasidegenerate states. These states are inhomogeneous configurations corresponding to excited states in the MFA that are nearly degenerate in energy with the naive MFA ground state. They contribute substantially to the actual quantum ground state through quantum tunneling. The sawtooth map emerged after the mixing of these quasidegenerate states were taken into account in Ref. [7].

More recently, a different approach was proposed in Ref. [8] that uses a generalized squeezed state many-body wave function to demonstrate that the sawtooth behavior is simply the result of quantum fluctuations. Similar to Ref. [7], this paper also adopted an approximation that goes beyond the MFA. In our opinion, the approach of Ref. [8] is very appealing in principle. However, we believe that some difficulties in this paper need be overcome before it could be considered satisfactory. First, the assumed squeezed state many-body ground state is general enough so as to include the correlations of the positions of the atoms, expressed by the covariances $G_{ij}=\langle(x_i-\overline{x_i})(x_j-\overline{x_j})\rangle$ $(i\neq j)$, where x_i is the position of the ith atom, $\langle\cdots\rangle$ is the expectation value in a given quantum state, and $\overline{x_i}=\langle x_i\rangle$. However, to find the equilibrium state of the model, one has to solve a system of coupled equations of the variables x_i and the G_{ij} obtained in Ref. [8] by varying x_i and G_{ij} independently. The equations obtained are so complicated that the task of solving them within a single numerical framework is very difficult. In fact, in Ref. [8] a hybrid numerical analysis was adopted in which the equations for the G_{ij} were not solved. Instead, the values of G_{ij} were taken from QMC data. These values were then treated as initial conditions in solving the equations for the atomic positions x_i's. Technically, such hybrid analysis is not satisfactory. Second, the covariance terms G_{ij} $(i\neq j)$ are constrained by the values of the fluctuation terms G_{ii} and G_{jj} through the Cauchy-Schwarz inequality. These constraints guarantee the boundedness from below of the effective Hamiltonian [9]. But this also calls for a proper variational principle that has to take care of the interdependence of the G_{ij} terms.

*Mailing address: Department of Physics, Tamkang University, Tamsui 25137, Taiwan.

In this paper we shall show that all the essential features observed in the QMC studies can in fact be obtained from an independent-particle picture of the many-body ground state, i.e., in the MFA. In the independent-particle picture the many-body trial wave function is factorizable into single-particle states. One can assume the single-particle state to have the form of a squeeze state. For the quantum FK model, a simpler and, in our view, more elegant approach is to adopt Dirac's time-dependent variational principle [10] together with the Jackiw-Kerman (JK) function [11] as the single-particle state. This is the main difference between our approach and the naive MFA in Ref. [7], where the single-particle wave functions were determined by solving a set of self-consistency conditions. We shall show that our simple independent-particle approach produces an effective classical Hamiltonian that is bounded from below, admits simple numerical solution of the ground state without recourse to QMC analysis, and reproduces the essential features observed in QMC studies.

II. EFFECTIVE HAMILTONIAN

The Hamiltonian of the quantum FK model is given by

$$\mathcal{H}=\sum_i \left[\frac{\hat{p}_i^2}{2m}+\frac{\gamma}{2}(\hat{q}_{i+1}-\hat{q}_i)^2-V\cos(l_0\hat{q}_i)\right]. \tag{1}$$

Here $\hat{q}_i$ and $\hat{p}_i$ are the position and momentum operators, respectively, of the ith atom, γ the elastic constant of the spring, and V and $2\pi/l_0$ are the strength and the period of the external potential. As in Ref. [7], it is convenient to use the dimensionless variables $\hat{Q}_i=l_0\hat{q}_i$, $\hat{P}_i=l_0\hat{p}_i/\sqrt{m\gamma}$, and $K=Vl_0^2/\gamma$. With these new variables, we obtain the following dimensionless Hamiltonian H

$$H=\sum_i \left[\frac{\hat{P}_i^2}{2}+\frac{1}{2}(\hat{Q}_{i+1}-\hat{Q}_i)^2-K\cos(\hat{Q}_i)\right]. \tag{2}$$

We have $\mathcal{H}=\gamma H/l_0^2$. The effective Planck constant is $\tilde{\hbar}=\hbar l_0^2/\sqrt{m\gamma}$. For the classical FK model, the Aubry transition occurs at the critical value $K_c=0.971635\ldots$.

To study the ground-state properties of the quantum FK model in Eq. (2), we adopt here the time-dependent variational principle pioneered by Dirac [10]. In this approach, one first constructs the effective action $\Gamma=\int dt\langle\Psi,t|i\hbar\partial_t-\mathcal{H}|\Psi,t\rangle$ for a given system described by $\mathcal{H}$ and $|\Psi,t\rangle$. Variation of Γ is then the quantum analogue of the Hamilton's principle. The time-dependent Hartree-Fock approximation emerges when a specific ansatz is made for the state $|\Psi,t\rangle$. We now assume the trial wave function of the ground state of our quantum FK system to have the Hartree form $|\Psi,t\rangle=\Pi_i|\psi_i,t\rangle$, where the normalized single-particle state $|\psi_i,t\rangle$ is taken to be the JK wave function [11]:

$$\langle Q_i|\psi_i,t\rangle=\frac{1}{(2\pi\tilde{\hbar}G_i)^{1/4}}\times\exp\left\{-\frac{1}{2\tilde{\hbar}}(Q_i-x_i)^2\left[\frac{1}{2}G_i^{-1}-2i\Pi_i\right]+\frac{i}{\tilde{\hbar}}p_i(Q_i-x_i)\right\}. \tag{3}$$

The real quantities $x_i(t)$, $p_i(t)$, $G_i(t)$, and $\Pi_i(t)$ are variational parameters the variations of which at $t=\pm\infty$ are assumed to vanish. The JK wave function can be viewed as the Q representation of the squeeze state [12]. We prefer to use the JK form since the physical meaning of the variational parameters contained in the JK wave function is most transparent, as we shall show below. Furthermore, the JK form is in the general Gaussian form so that integrations are most easily performed.

It is not hard to check that x_i and p_i are the expectation values of the operators $\hat{Q}_i$ and $\hat{P}_i$: $x_i=\langle\Psi|\hat{Q}_i|\Psi\rangle$, $p_i=\langle\Psi|\hat{P}_i|\Psi\rangle$. Also, one has $\langle\Psi|(\hat{Q}_i-x_i)^2|\Psi\rangle=\tilde{\hbar}G_i$, and $\langle\Psi|i\tilde{\hbar}\partial_t|\Psi\rangle=\Sigma_i(p_i\dot{x}_i-\tilde{\hbar}G_i\dot{\Pi}_i)$, where the dot represents a derivative with respect to time t. It is now clear that $\tilde{\hbar}G_i$ is the mean fluctuation of the position of the ith atom, and that $G_i>0$. With these expectation values, the (rescaled) effective action Γ for the dimensionless H can be worked out to be $\Gamma(x,p,G,\Pi)=\int dt[\Sigma_i\omega_0^{-1}(p_i\dot{x}_i+\tilde{\hbar}\Pi_i\dot{G}_i)-H_{eff}]$, where $\omega_0=\sqrt{\gamma/m}$ is the angular frequency of the spring, and $H_{eff}=\langle\Psi|H|\Psi\rangle$ is the effective Hamiltonian given by

$$H_{eff}=\sum_i\frac{1}{2}\left[p_i^2+\tilde{\hbar}\left(\frac{1}{4}G_i^{-1}+4\Pi_i^2G_i\right)\right]+\sum_i\frac{1}{2}(x_{i+1}-x_i)^2+\sum_i\frac{\tilde{\hbar}}{2}(G_{i+1}+G_i)-\sum_i K\exp\left(-\frac{\tilde{\hbar}}{2}G_i\right)\cos x_i. \tag{4}$$

The last term in Eq. (4) can be very easily obtained from $\langle\Psi|F(Q_i)|\Psi\rangle=\Sigma_{m=0}^{\infty}F^{(2m)}(x_i)(\tilde{\hbar}G_i)^m/(2m)!!$, where $F^{(n)}(x)=\partial^nF(x)/\partial x^n$, and $n!!\equiv n(n-2)(n-4)\ldots1$. Equation (4) is bounded from below. One sees from the form of the effective action Γ that Π_i is the canonical conjugate of G_i.

Varying Γ with respect to x, p, G, and Π then gives the equations of motion in the Hartree-Fock approximation. Since we are mainly concerned with the static properties of the ground state of the quantum FK model, we must set the time derivatives of these variables to zero. This gives the equations that determine the values of variational parameters corresponding to the equilibrium states (which include the ground state). Equivalently, we can obtain the equations for the equilibrium states by directly varying the effective Hamiltonian H_{eff} with respect to the variables. Varying H_{eff} with respect to p_i, Π_i, x_i, and G_i give, respectively,

$$p_i=0, \quad 4\Pi_i G_i=0, \tag{5}$$

$$x_{i+1}-2x_i+x_{i-1}=K\exp\left(-\frac{\tilde{\hbar}}{2}G_i\right)\sin x_i, \tag{6}$$

$$\frac{1}{4}G_i^{-2}-K\exp\left(-\frac{\tilde{\hbar}}{2}G_i\right)\cos x_i-2=4\Pi_i^2. \tag{7}$$

The second equation in Eq. (5) implies $\Pi_i=0$ as $G_i>0$. This in turn means that the right-hand side of Eq. (7) is equal to zero:

$$\frac{1}{4}G_i^{-2}-K\exp\left(-\frac{\tilde{\hbar}}{2}G_i\right)\cos(x_i)-2=0. \tag{8}$$

In the limit $\hbar=0$, Eq. (6) is equivalent to the standard map. We note that Eq. (6) was also obtained in Ref. [8]. This is because in the formulation in Ref. [8] the covariances G_{ij}'s decoupled from the x_i and the fluctuations G_{ii} (G_i in our case) in the variation of their Hamiltonian with respect to x_i. Unlike our case, of course, these covariance terms do actually influence the solutions of Eq. (6) through other equations obtained by variation of the Hamiltonian with respect to the G_{ii} and G_{ij}. And it is these equations that caused the difficulties mentioned in the Introduction. In particular, the values of the G_{ii} were input from the QMC data in order to solve for the x_i in Eq. (6). Our simple approach, on the other hand, allows us to solve for both the values of x_i and G_i coupled by Eqs. (6) and (8) consistently by a single numerical method.

From $p_i=\Pi_i=0$ and Eq. (4), we see that the problem of finding the static ground state of the quantum FK model reduces to the problem of minimizing with respect to x_i and G_i the following effective potential:

$$V_{eff}=\sum_i \frac{1}{2}(x_{i+1}-x_i)^2+\sum_i \frac{\tilde{\hbar}}{8}G_i^{-1} + \sum_i \frac{\tilde{\hbar}}{2}(G_{i+1}+G_i)-\sum_i K\exp\left(-\frac{\tilde{\hbar}}{2}G_i\right)\cos x_i. \tag{9}$$

Equations (6) and (8) are just the conditions $\partial V_{eff}/\partial x_i=0$ and $\partial V_{eff}/\partial G_i=0$, respectively.

III. NUMERICAL RESULTS

We numerically solve for the set of variables x_i and G_i, which characterize the ground state using the Newton method [13]. In all our numerical computations the winding number $P/Q=610/987$, which is an approximation of the golden mean winding number $(\sqrt{5}-1)/2$, is used with the periodic boundary condition $x_{i+Q}=x_i+2\pi P$ [14]. This winding number is much more accurate than those used in previous works to approximate the golden mean number, thus giving us better accuracy in the computations of physical quantities related to the ground state. We emphasize that all values of x_i and G_i are determined by the same numerical method consistently. In particular, we do not have to input the values of G_i from quantum Monte Carlo results in order to solve for x_i.

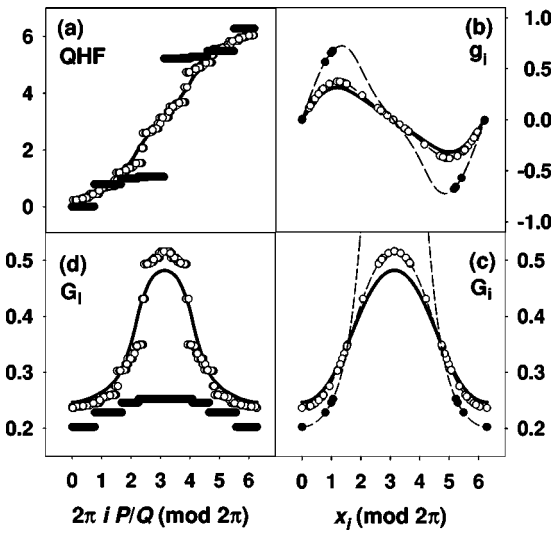

FIG. 1. Structure of the quantum ground state for $K=5$ and winding number $P/Q=610/987$ at $\tilde{\hbar}=2$ (black dots), 6 (white dots), and 7 (black curve). (a) quantum hull function plotted against unperturbed atomic positions; (b) g function plotted against actual atomic positions (the dashed curves represent Eq. (11) with G_i satisfying Eq. (8); (c) and (d) quantum fluctuations G_i plotted against the actual and unperturbed positions, respectively. The dashed curves in (c) represent the curves of Eq. (8) for different $\tilde{\hbar}$.

Having obtained the values of x_i which give the mean positions of the quantum atoms in the chain, we can compare the results with the classical configuration, following Ref. [6], in two ways: (1) by the quantum hull function, which is the plot of $x_i \pmod{2\pi}$ of the atoms against their unperturbed positions $2\pi iP/Q \pmod{2\pi}$ and (2) by the so-called g function, defined by

$$g_i \equiv K^{-1}(x_{i+1}-2x_i+x_{i-1}), \tag{10}$$

versus the actual atomic positions x_i. From Eq. (6), we also have

$$g_i=\exp\left(-\frac{\tilde{\hbar}}{2}G_i\right)\sin x_i. \tag{11}$$

Here G_i is related to x_i by Eq. (8). We see from this equation that quantum fluctuations G_i will modify the shape of the classical *sine* map. In addition to these two types of graphs, we also plot the graph of G_i against the unperturbed and the actual positions. The formal graph was first introduced in Ref. [6] to show the strong correlation of the fluctuations of atoms' positions with their unperturbed positions. We introduce the latter type of graphs here since we think that such graphs provide a better picture about how the quantum fluctuations of the atoms are related to their actual positions.

In Fig. 1 we show the four graphs mentioned above with

different values of $\tilde{\hbar}$ for the supercritical case $K=5$. Figure 1(a) shows the quantum hull functions. For small values of $\tilde{\hbar}$ the quantum hull function consists of a countable set of steps discontinuities, just as in the classical case: the atoms are in a pinning phase. In fact, the atoms are more likely to be located near the valley of the external potential well, namely, near $x_i=0 \pmod{2\pi}$. As the quantum effect increases, i.e., for increasing values of $\tilde{\hbar}$, the quantum hull function gradually changes into a monotonic analytic function, signifying that the system is entering the depinning phase. There exists a critical value, approximately $\tilde{\hbar}_c=6.58$ for $K=5$, above which the quantum hull function changes from an nonanalytic function to an analytic one. This is a quantum analogue of the Aubry transition in the classical case, and can therefore be called the quantum Aubry transition.

Next in Fig. 1(b) we show the graphs of the g function. The curve defined by Eq. (11) with G_i satisfying Eq. (8) are shown here as dashed curves for different $\tilde{\hbar}$. In the classical limit ($\tilde{\hbar}=0$) this curve is simply the standard map (*sine* curve). As $\tilde{\hbar}$ increases, the amplitude of the curve decreases. For sufficiently large $\tilde{\hbar}$, the curve resembles more closely a ''sawtooth'' shape. This is first noted in QMC study in Ref. [6]. Here we see that it comes out very naturally from the equation of motions (8) and (11). We have therefore demonstrated that the sawtooth map could be recovered in the MFA. In the supercritical case ($K=5$), when $\tilde{\hbar}<\tilde{\hbar}_c$, the positions x_i of the atoms cover only a subset of the g curves. This is in accord with the fact that the atoms are in the pinning phase [cf. Fig. 1(a)]. As $\tilde{\hbar}$ increases, the points begin to spread along the g curve. When $\tilde{\hbar}>\tilde{\hbar}_c$, the g graph is completely covered as the system has entered the depinning phase.

Figure 1(c) shows the quantum fluctuations G_i plotted against the actual atomic positions x_i. The dashed curves represent the curves of Eq. (8) for different $\tilde{\hbar}$. For small $\tilde{\hbar}$, the atoms are located near $x_i=0 \pmod{2\pi}$ with small values of G_i, which means, from Eq. (3), that the wave functions are highly peaked at these positions. As the quantum effect increases, the external potential is so modified that now the atoms could be found at other positions, but with atoms at $x_i=\pi \pmod{2\pi}$ having the largest value of G_i. This indicates that wave functions of the atoms near the top of the potential are more extended with smaller amplitudes. Again, when $\tilde{\hbar}>\tilde{\hbar}_c$, the curves of Eq. (8) are completely covered by the solutions x_i. To compare with the results in Ref. [6], we plot the values of G_i against the unperturbed positions in Fig. 1(d). One sees that the values of G_i are strongly correlated with the unperturbed positions, as first noted in Ref. [6]. For $\tilde{\hbar}<\tilde{\hbar}_c$ the graphs consists of steps discontinuities, and for $\tilde{\hbar}>\tilde{\hbar}_c$ the graphs are continuous. This is correlated with the graphs of the quantum hull function in Fig. 1(a), since from Eq. (8) any fixed value of x_i corresponds to a fixed value of G_i.

Next we show in Fig. 2 the corresponding graphs for the case $K=1.5$. This represents the situation that is slightly over the critical classical case. The general trends of the behavior of the graphs are the same as those in Fig. 1. As expected, quantum Aubry transition takes place at a smaller $\tilde{\hbar}_c=1.17$. We note here that the shape of the g function at large $\tilde{\hbar}$ in this case is intermediate between a *sine* and a sawtooth map.

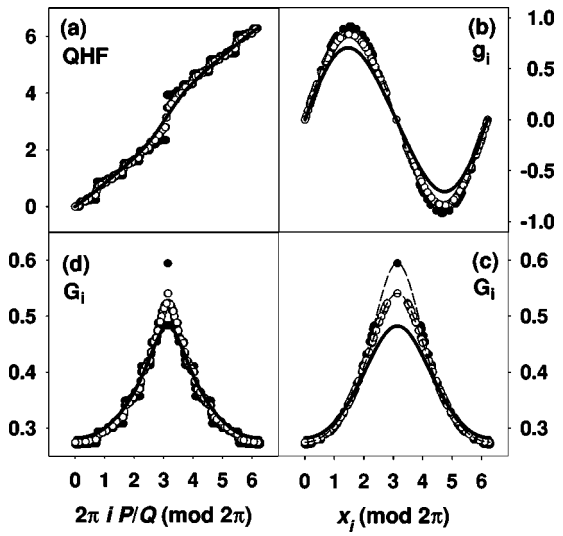

FIG. 2. Same as Fig. 1 for $K=1.5$ and $\tilde{\hbar}=0.5$ (black dots), 1.0 (white dots), and 2 (black curve).

We have also checked the subcritical cases with $K<K_c$. The classical system is already in the depinning phase in this regime. Quantum fluctuations only enhance the trend of depinning. The g function is found to be closer to a *sine* shape with smaller amplitude for higher $\tilde{\hbar}$. This is consistent with the QMC results [6].

Finally, we note here that, while we have reproduced the essential features first observed in the QMC studies of the quantum FK model, there is also slight discrepancy between the results of these two approaches. The difference is that, for a fixed value of K, the QMC results [6] indicated that the sawtooth shape of the g function appeared at a lower value of $\tilde{\hbar}$, and that the atoms began to spread along the g curve also at a smaller $\tilde{\hbar}$. For example, at $K=5$ the QMC results showed that the above situation already appeared at $\tilde{\hbar}=0.2$, while our results [cf. Fig. 1(b)] indicate that at $K=5$ and at a higher $\tilde{\hbar}=2$, the system is still closer to the classical case. We believe this could be explained as follows. First, our independent-particle wave function is only the lowest-order approximation of the many-body wave function of the quantum FK system. A more accurate description of the system will require a better assumption of the wave function than that assumed here. This presumably may require the inclusion of the effects of the covariance terms as advocated in Ref. [8], but with a more appropriate variational principle to circumvent the difficulties already mentioned in the Introduction. Second, our results are obtained at zero temperature, while those in the QMC analysis were obtained, by the nature of the method itself, at small but finite temperatures (temperature $T=0.0067$ as given in Ref. [6]). It is natural that thermal fluctuations will cause the atoms to spread away from their zero-temperature positions.

IV. SUMMARY

In conclusion, we have presented a simple and complete variational approach to the quantum FK model based on a Hartree-type many-body trial wave function of the JK form. The effective Hamiltonian obtained is bounded from below, and is simple enough for a complete numerical solution for the static ground state of the model in various quantum regimes. Numerical results show that our simple approach captures the essence of the quantum effects first observed in QMC studies. The map appropriate for the quantum FK model is well described by Eqs. (11) and (8). In contrast to previous approaches, we do not require the existence of the complicated quasidegenerate states, or the partial help from QMC data in order to obtain these results.

ACKNOWLEDGMENTS

This work is supported in part by the R.O.C Grant No. NSC 89-2112-M-032-004. Part of the work was done while one of us (C.L.H.) was visiting the Theory Division at KEK (Japan) under the auspices of the exchange program between KEK (Japan) and the National Center for Theoretical Sciences (Taiwan). He would like to thank the staff and members of the theory group of KEK for their hospitality and support. After the paper was submitted, we were kindly informed by Professor B. Hu that he and W M. Zhang in their previous incomplete work [15] had obtained a Hamiltonian similar to our Eq. (4), but that they had not studied the ground-state properties.

[1] Y.I. Frenkel and T. Kontorova, Zh. Éksp. Teor. Fiz. **8**, 1340 (1938) [Sov. Phys. JETP **13**, 1 (1938)].

[2] F.C. Frank and J.H. van der Merwe, Proc. R. Soc. London, Ser. A **198**, 205 (1949).

[3] P. Bak, Rep. Prog. Phys. **45**, 587 (1982).

[4] S. Aubry, in *Solitons and Condensed Matter Physics*, edited by A.R. Bishop and T. Schneider (Springer-Verlag, Berlin, 1978); J. Phys. (France) **44**, 147 (1983); Physica D **7**, 240 (1983); **8**, 381 (1983).

[5] M.G. Rozman, M. Urbakh, and J. Klafter, Phys. Rev. Lett. **77**, 683 (1996); Phys. Rev. E **54**, 6485 (1996); M. Weiss and F.-J. Elmer, Phys. Rev. B **53**, 7539 (1996); T. Gyalog and H. Thomas, Europhys. Lett. **37**, 195 (1996).

[6] F. Borgonovi, I. Guarneri, and D. Shepelyansky, Phys. Rev. Lett. **63**, 2010 (1989); Z. Phys. B: Condens. Matter **79**, 133 (1990); F. Borgonovi, Ph.D. dissertation, Universitá Degli Studi di Pavia, 1989, unpublished.

[7] G.P. Berman, E.N. Bulgakov, and D.K. Campbell, Phys. Rev. B **49**, 8212 (1994).

[8] B. Hu, B. Li, and W.-M. Zhang, Phys. Rev. E **58**, 4068 (1998); B. Hu and B. Li, Physica A (to be published).

[9] B. Hu and B. Li, private communications.

[10] P.A.M. Dirac, Proc. Cambridge Philos. Soc. **26**, 376 (1930).

[11] R. Jackiw and A. Kerman, Phys. Lett. A **71**, 158 (1979).

[12] Y. Tsue and Y. Fujiwara, Prog. Theor. Phys. **86**, 443 (1991).

[13] H.J. Schellnhuber, H. Urbschat, and A. Block, Phys. Rev. A **33**, 2856 (1986); H.J. Schellnhuber, H. Urbschat, and J. Wilbrink, Z. Phys. B: Condens. Matter **80**, 305 (1990).

[14] This is in accord with Ref. [8] and different from Ref. [7], which set $x_0=0$, $x_Q=2\pi P$. It was mentioned in Ref. [8] that their QMC results for these two boundary conditions were slightly different.

[15] B. Hu, in *Proceedings of the 4th Drexel Conference on Quantum Nonintegrability*, edited by D.H. Feng and B.L. Hu (Drexel University, Philadelphia, 1997). In a brief section of this paper a Hamiltonian very similar to our Eq. (4) (but with a fixed $\tilde{\hbar}=1$) was presented based on squeezed state approach.